

Yiwen Xu and M. L. Wesely *
Environmental Research Division, Argonne National Laboratory, Argonne, Illinois

1. INTRODUCTION

Dry deposition is an important process of ozone (O_3) removal from the atmosphere. Most chemical transport models or photochemistry models use the traditional three-resistance model to simulate dry deposition. The treatment of the resistance used to describe uptake by plant stomata, which can be the major pathway for surface uptake of O_3 , varies considerably among the models. In the Regional Acid Deposition Model (RADM) and the Urban Airshed Model (UAM), stomatal resistance is estimated by empirical formulations and parameters assigned on the basis of 11 land use types (Wesely 1989) and 5 seasonal categories. In this study, our goal is to examine the effects of dry deposition on regional-scale O_3 concentration and transport. The photochemistry model in the UAM/Comprehensive Air Quality Model with Extensions (CAMx; Environ 1998) is used to resimulate O_3 surface concentrations in the eastern United States for a past Ozone Transport Assessment Group (OTAG) study case (OTAG 1997). The photochemistry model was modified with a dry deposition scheme in which the bulk canopy stomatal resistance is estimated by leaf area index (LAI) inferred from satellite remote sensing data (Gao 1995; Gao and Wesely 1995). This method can significantly improve the estimates of bulk canopy stomatal resistance in large-scale simulations. The resulting O_3 concentration distributions were analyzed for the model domain over the eastern United States.

2. PHOTOCHEMISTRY AND DEPOSITION MODELS

The photochemistry model is an Eulerian model with a plume-in-grid submodel. This model simulates the emission, dispersion, and removal of pollutants in the lower troposphere for each chemical species. Dry deposition is usually treated as a first-order removal mechanism, where the flux of a chemical species to the surface is the product of a characteristic deposition velocity and its concentration in the surface layer. In the CAMx model, dry deposition is not explicitly treated as a separate process in the time-splitting approach. Instead, deposition velocities for each species, calculated on the basis of their chemical properties and the surface

meteorological conditions, are used to specify the lower condition for vertical diffusion.

Dry deposition velocities are derived by using the three-resistance model described by Wesely (1989). The aerodynamic resistance represents bulk transport through the lowest several meters by turbulent diffusion. The quasi-laminar sublayer (boundary) resistance represents molecular diffusion through the layer of air directly in contact with the particular surface to which pollutants are being deposited. The stomatal resistance is expressed as several serial and parallel resistances that depend on the physiological, physical, and chemical characteristics of the leaves. Many of the resistances are dependent on season and land use; some of the resistances need to be adjusted for solar insolation, moisture stress, and surface wetness. The bulk canopy stomatal resistance for species i can be expressed as

$$R_{si} = \frac{D_{H_2O}}{D_i} R_{sim} \frac{1 + [200(G + 0.1)]^{-1}]^2}{400[T_s(40 - T_s)]} \quad (1)$$

Here R_{sim} is the minimum bulk canopy stomatal resistance for water vapor, G is the solar irradiation, T_s is the surface air temperature, D_i is the molecular diffusivity of gas i in air, and D_{H_2O} is the molecular diffusivity for water vapor. Other uptake pathways at the surface, the role of solubility, and chemical reactivity (oxidation of biological substances) affecting uptake by different chemical species are described with various parameterizations. As has been noted previously (Xu and Wesely 1999), a limitation of the approach described by Wesely (1989) is that its reliance on preset land use and seasonal categories can result in descriptions of uptake properties that do not vary realistically in time and space. The following section is an introduction to use of the dry deposition scheme with satellite remote sensing data to detect surface vegetation and characteristics, as well as implementation of the scheme with the chemistry model. The focus is on the evaluation of bulk canopy stomatal resistance. Other components of surface resistances and conductances are estimated with the procedures described by Wesely (1989).

3. USE OF SATELLITE OBSERVATIONS

The evaluation of bulk canopy stomatal resistance involves modeling of LAI and absorbed

* Corresponding author address: Marvin L. Wesely, Environmental Research Division, Argonne, IL 60439 USA; e-mail: mlwesely@anl.gov

photosynthetically active radiation (PAR) derived by using satellite data on reflected surface radiances detected in channels 1 (red band, with wavelengths of 0.58-0.68 μm) and 2 (near-infrared band, 0.71-0.98 μm) of advanced very high resolution radiometers (AVHRRs) on National Oceanic and Atmospheric Administration (NOAA) polar-orbiting environmental satellites. Monthly composites of 8-km-resolution data from NOAA's Pathfinder Land Data Set were used (Agbu and James 1994). For the canopy-soil system, an increasing amount of green leaves results in a decrease in the total canopy reflectance in the red band and an increase in total canopy reflectance in the near-infrared band. Gao (1995) and Gao and Wesely (1995) used a series of radiative transfer equations to describe the behavior of light in canopy-soil systems, starting with an equation for the wavelength-dependent reflectance of the bulk surface,

$$\rho = \frac{(\rho_s \rho_m - 1) + (1 - \rho_s / \rho_m)(1 - P)^{2K}}{(\rho_s - 1 / \rho_m) + (\rho_m - \rho_s)(1 - P)^{-2K}}, \quad (2)$$

where the probability P of light penetration through the canopy can be expressed as

$$P = \exp[-G(\theta)\Omega L_T / \cos \theta]. \quad (3)$$

Here ρ_r and ρ_m are the wavelength-dependent reflectances for soil and the bulk canopy, respectively, and K is the wavelength-dependent extinction coefficient for the bulk canopy. A set of empirical formulas for K and ρ_m were derived by Goudriaan (1977) to approximate the numerical solution that describes the complicated interaction of leaf scattering coefficients, leaf angle distribution, and solar zenith angle. $G(\theta)$ is the mean projection of unit leaf area on the plane perpendicular to the solar beam at zenith angle θ , L_T is the LAI for the total canopy, and Ω is the canopy clumping index. The values of ρ_r and Ω are estimates based on studies reported in the scientific literature. L_T and ρ for the red $\rho(r)$ and near-infrared $\rho(n)$ bands are found by iterations in which (1) and (2) are solved, and values of the normalized difference vegetation index, $\text{NDVI} = [\rho(n) - \rho(r)] / [\rho(n) + \rho(r)]$ or simple ratio, $\text{SR} = \rho(n) / \rho(r)$, match those measured by AVHRRs on satellites.

For a canopy with a spherical leaf angle distribution, the PAR within the canopy can be computed as

$$I_{PAR} = I_{PAR0} \exp(-KL), \quad (4)$$

where L is the cumulative LAI above the height of interest, and I_{PAR0} is the incident PAR above the canopy.

Plant leaf stomata provide the dominant pathway for the dry deposition of trace gases that are moderately soluble in water or highly reactive with substances in

substomatal cavities. Although reactions with external plant surfaces and surface elements at the ground are important sites of O_3 destruction, most of the daytime removal of these species by vegetative canopies is accomplished by destruction in leaf substomatal cavities. The substomatal resistance of O_3 uptake in the leaf mesophyll cells is very small; it has been shown by many studies to be practically zero. The transfer velocity or conductance through the stomata is regulated by the aperture size, location, and number of stomata. We estimate the bulk canopy stomatal conductance G_{si} (inverse of resistance R_{si}) for gas species i as

$$G_{si} = \int_0^{L_T} w_s g_{si} dL, \quad (5)$$

where w_s represents the effects of variations in environmental factors on stomatal conductance within the canopy. The term g_{si} represents the stomatal conductance for individual leaves and is dependent on absorbed PAR, air vapor pressure deficit δe , and soil moisture content θ_s :

$$g_{si} = \frac{D_i}{D_{H_2O}} [\alpha_1 I_{PAR} / (\alpha_2 + I_{PAR})] f_1(\delta e) f_2(\theta_s). \quad (6)$$

In (6), D_i is the molecular diffusivity in air of the substance of interest, D_{H_2O} is the molecular diffusivity of water vapor, and α_1 and α_2 are empirical constants. As Gao and Wesely (1995) showed, inserting (4) into (6) and then integrating the resulting expression according to (5) yields an analytical expression for G_{si} . Hence, estimates of G_{si} are made effectively on the basis of L_T and absorbed PAR inferred from satellite data.

4. RESULTS AND DISCUSSION

The CAMx photochemistry model, modified by incorporation of the new dry deposition scheme, was used to generate O_3 concentration maps for 7 July 1995 over the eastern United States. The purpose of these simulations was to analyze O_3 formation in relation to anthropogenic and natural emission sources and the chemical and physical processes of O_3 removal. The relation of O_3 formation to biogenic emissions, anthropogenic emission of NO_x , and meteorological factors can be found in the previous study by Xu et al. (2002). The present study focuses on O_3 dry deposition and its effects on the spatial distribution of O_3 concentrations.

The modified photochemistry model was applied within a time step of 1 h and a minimum horizontal grid size of 36 km or 12 km, which matched the time steps and sizes of RAMS (Regional Atmospheric Modeling System; Pielke et al. 1992) meteorological output. The domain of the relatively coarse, 36-km grid extended from 99° to 67°W and from 26° to 47°N; the nested, relatively fine, 12-km grid extended from 92° to 69.5°W

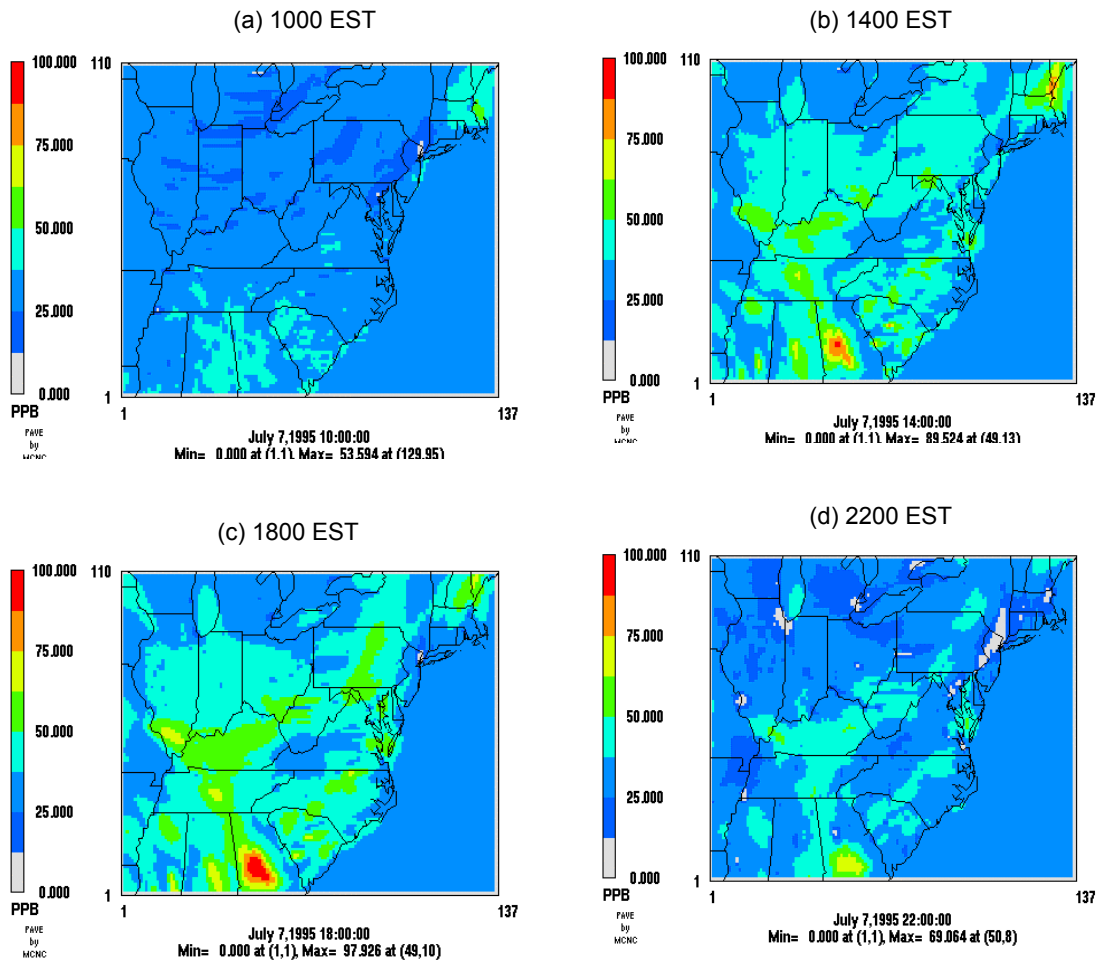


FIG. 1. Near-surface O₃ concentrations simulated for the eastern United States with the dry deposition scheme that uses satellite remote sensing data, for four times on 7 July 1995.

and from 32° to 44°N. RAMS was used to generate estimates of wind speed, temperature, pressure, precipitation, humidity, cloud height, cloud cover, and vertical turbulence coefficients. Hourly emission rates for biogenic isoprene, anthropogenic NO_x, and other gas species, including emissions from large point sources, were obtained from the original OTAG emission inventory (OTAG 1997).

Simulated O₃ concentrations obtained with the new dry deposition scheme are presented in Fig. 1. The selected distributions at 1000 EST, 1400 EST, 1800 EST, and 2200 EST show typical variations in O₃ concentration, including a mid-afternoon peak and a nighttime minimum. The O₃ concentration in most areas at 1000 EST was quite low (25 ppb), except in southern states (Georgia, Alabama, and South Carolina) and a northeastern state (Massachusetts), where O₃ concentrations were about 50 ppb. Figure 1b shows that

O₃ concentrations increased during the early afternoon in most of the southeastern United States and in northeastern states; in some areas of Georgia and Massachusetts, the O₃ concentration had already reached 100 ppb. At 1800 EST, somewhat higher O₃ concentrations formed in the middle of the domain. Peaks in concentrations appeared in Illinois, Tennessee, Mississippi, Alabama, Georgia, and New England. The maximum value was approximately 100 ppb, in Georgia (Fig. 1c). The ozone dissipated at night, as indicated by the distributions of O₃ concentrations at 2200 EST (Fig. 1d).

The diurnal cycle of O₃ in the lower planetary boundary layer (PBL) is dominated by photochemical reactions during the daytime and by chemical destruction and dry deposition at night. The presence of ultraviolet radiation, together with emissions of NO_x and volatile organic compounds (VOCs), contributes to the

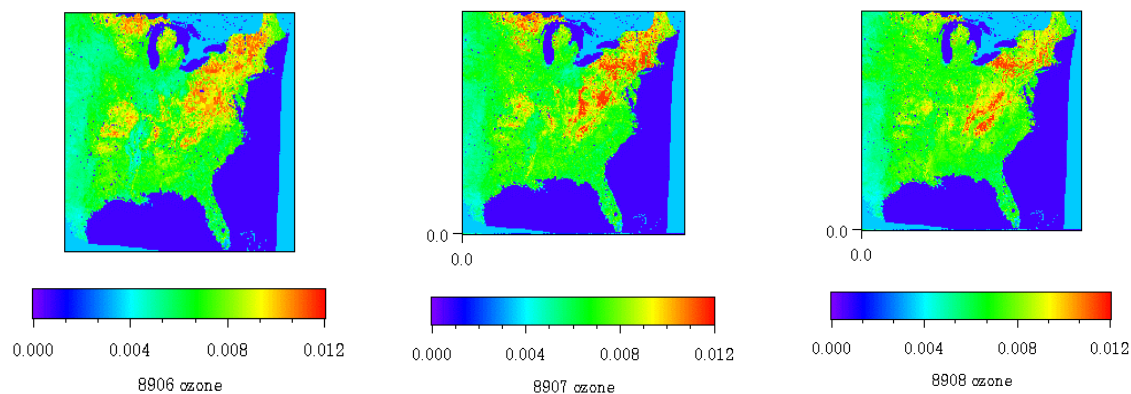


FIG. 2. Estimates of O_3 dry deposition velocity ($m s^{-1}$) at noon under mostly cloudless skies in the eastern half of the United States for June (left), July (center), and August (right) of 1989, made with the dry deposition scheme that uses satellite remote sensing data.

photochemical production of O_3 . As used here, CAMx neglected O_3 entrainment from the upper troposphere, which usually is small. During the night and early morning, the PBL is usually thermally stratified as a result of surface cooling, and mixing of O_3 from the upper mixed layer into air close to the ground can be suppressed, resulting in depletion of O_3 near the surface by dry deposition and reactions with local emissions of NO. Accurate simulation of vertical mixing in the PBL in extremely stable conditions and the associated rapid depletion of O_3 is difficult, but the nighttime O_3 concentrations appear to have been depicted without readily detectable misrepresentation by CAMx for the late morning and evening (Figs. 1a and 1d).

Because O_3 is a strong oxidant, it is removed efficiently by the substomatal mesophyll region of leaves during the daytime when the plant stomata are open. Ozone dry deposition velocities have been widely studied through measurements and modeling activities and are commensurate with the values shown in Fig. 2, which were estimated with the present scheme for June, July, and August 1989. In summer over northern forests, the deposition velocity is usually about $0.1 cm s^{-1}$ at night, $0.8 cm s^{-1}$ in the morning, and $1.0 cm s^{-1}$ at noon. The value decreases in the afternoon to about $0.6 cm s^{-1}$ (Xu and Wesely 1999). These results illustrate the detailed spatial variations of deposition velocity that can be discerned for the eastern United States by the present scheme with 1-km-resolution land use data and 8-km satellite data.

Figure 3 compares O_3 concentrations estimated by the present dry deposition approach to estimates made with the previous RADM method using fixed seasonal categories; both of the methods were implemented with the CAMx model. The concentration patterns for the two methods are similar in most of the region, but the

concentrations generated with the present approach in the northeastern United States are smaller than those generated with the RADM method. The difference originates from generation by (2)-(6) of larger G_{si} values for mixed forests than the corresponding values of inverse R_{si} generated via (1) in the RADM method, which results in larger deposition velocities and greater removal of O_3 . This effect might be more noticeable in the northeastern United States than in some of the southern areas because of the differences in isoprene concentrations. That is, where isoprene is less abundant (some locations in the Northeast), O_3 production is limited by low concentrations of VOCs, and thus the O_3 lost to dry deposition cannot be replaced quickly. In contrast, replacement rates are higher in areas where isoprene concentrations are large (e.g., in some of the southern states).

5. CONCLUSIONS

The CAMx photochemistry model was applied with both the RADM dry deposition model and a new scheme that uses satellite data to infer bulk canopy stomatal conductance. The latter approach produces more detailed spatial (and temporal) variations in dry deposition velocity estimates than does the former. The diurnal cycles and spatial patterns appear to be realistic. The spatial distribution of O_3 concentrations in the eastern United States generated when the new dry deposition scheme was applied are similar to the pattern obtained with the RADM dry deposition scheme, but the O_3 concentrations in northeastern United States are smaller around noon. This difference is associated with larger estimates of deposition velocity made for mixed forests where the production of O_3 tends to be limited by low concentrations of VOCs.

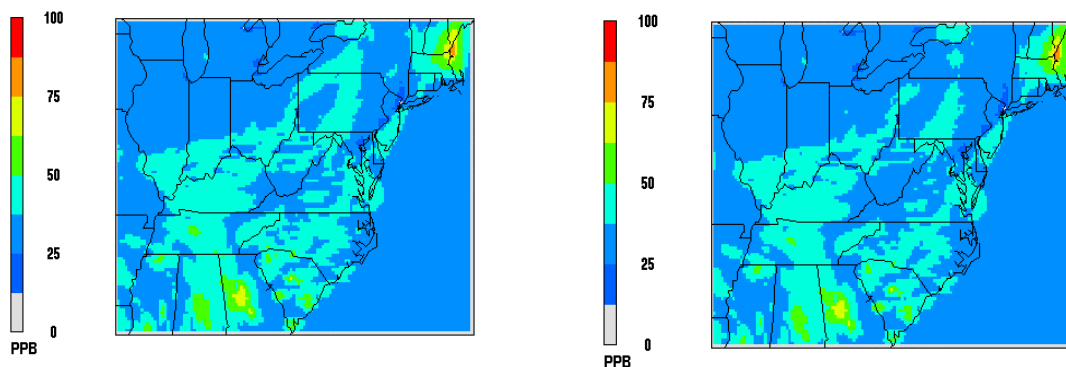


FIG. 3. Ozone concentrations computed with CAMx for 1200 EST on 7 July 1995 with (left) the RADM dry deposition scheme and (right) the new scheme relying on remote sensing data from satellites to infer green leaf area index.

Acknowledgments. This work was supported by the U.S. Department of Energy, Office of Science, Office of Biological and Environmental Research, Environmental Sciences Division, Atmospheric Chemistry Program, under contract W-31-109-Eng-38.

REFERENCES

- Agbu, P. A., and M. E. James, 1994: The NOAA/NASA Pathfinder AVHRR Land Data Set User's Manual. Goddard Distributed Active Archive Center, National Aeronautics and Space Administration, Goddard Space Flight Center, Greenbelt, MD, 104 pp. [Available online at http://daac.gsfc.nasa.gov/CAMPAIGN_DOCS/LAND_BIO/AVHRR_GD.pdf].
- Environ, 1998: CAMx User's Guide. Environ International Corporation, Navato, CA, 158 pp. [Available online at <http://www.camx.com/overview.html>]
- Gao, W., 1995: Modeling gaseous dry deposition over regional scales with satellite observations—I. Deriving surface conductances with AVHRR data. *Atmos. Environ.*, **29**, 739-747.
- Gao, W., and M. L. Wesely, 1995: Modeling gaseous dry deposition over regional scales with satellite observations—II. Model development. *Atmos. Environ.*, **29**, 727-737.
- Goudriaan J., 1977: Crop micrometeorology: A simulation study. Simulation Monographs, 257 pp. [Available from the Center for Agricultural Publishing Documentation (Pudoc), Wageningen, The Netherlands]
- OTAG, 1997: OTAG Technical Supporting Document, Final Report, Ozone Transport Assessment Group, U.S. Environmental Protection Agency, Office of Air Quality Planning & Standards, Technology Transfer Network [Available online at <http://www.epa.gov/ttn/rto/otag/finalrpt/>].
- Pielke, R. A., W. R. Cotton, R. L. Walko, C. J. Tremback, W. A. Lyons, L. D. Grasso, M. E. Nicholls, M. D. Moran, D. A. Wesley, T. J. Lee, and J. A. Copeland, 1992: A comprehensive meteorological modeling system—RAMS. *Meteor. Atmos. Phys.*, **49**, 69–71.
- Wesely, M. L., 1989: Parameterization of surface resistances to gaseous dry deposition in regional-scale numerical models. *Atmos. Environ.*, **23**, 1293-1304.
- Xu, Y., and M. L. Wesely, 1999: Modeling of dry deposition over regional scales with use of satellite data. *Preprints, Symposium on Interdisciplinary Issues in Atmospheric Chemistry*, Amer. Meteor. Soc., Boston, MA, 58-61.
- Xu, Y., M. L. Wesely, and T. E. Pierce, 2002: Estimates of biogenic emissions using satellite observations and influence of isoprene emission on O₃ formation over the eastern United States. *Atmos. Environ.* (in press).